Electronic Supplementary Material (ESI) for CrystEngComm.

Supporting Information

Dipole Field Driven Morphology Evolution in Biomimetic Vaterite

Heather F. Greer, Ming-Han Liu, Chung-Yuan Mou and Wuzong Zhou

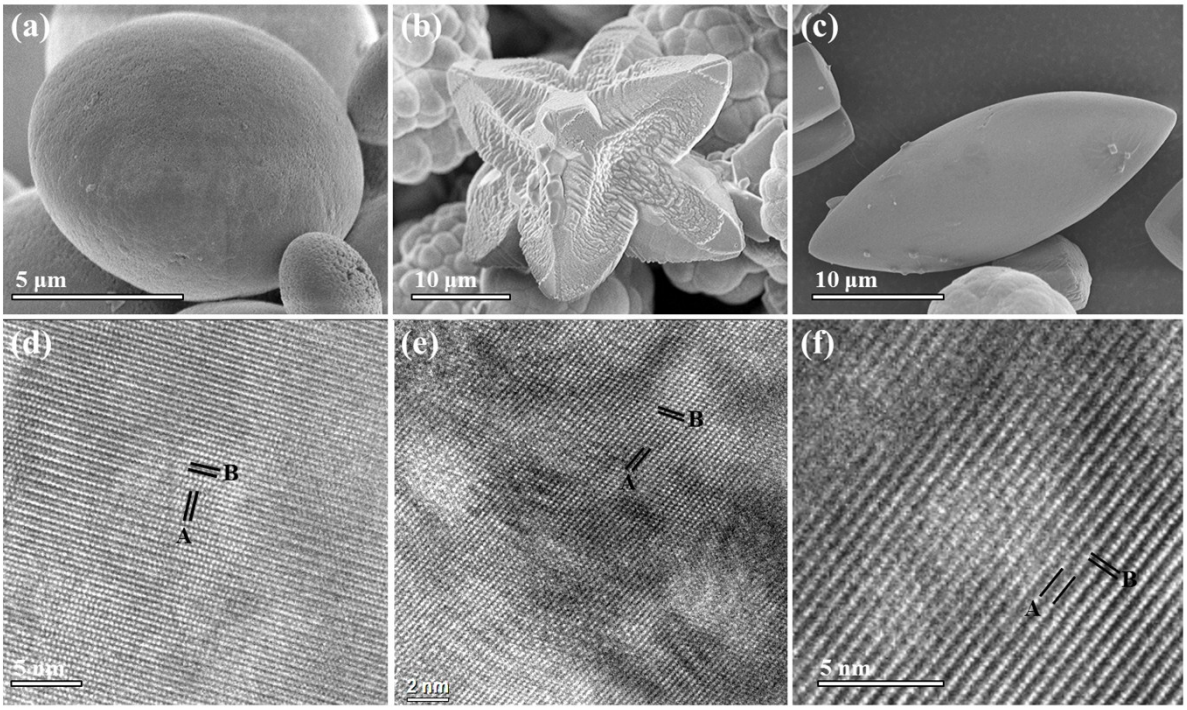

Fig. S1 SEM (a-c) and the corresponding HRTEM (d-f) images of the three different $CaCO_3$ polymorphs with characteristic morphologies present in the 3 h specimen. (a,d) Ellipsoidal hexagonal vaterite, (b,e) star-shaped rhombohedral calcite, and (c,f) spindle-shaped orthorhombic aragonite. The marked d-spacings, A: 3.54 Å and B: 4.14 Å in (d) can be indexed to the (100) and (002) planes of hexagonal vaterite. The d-spacings marked in (e) of A: 2.59 Å and B: 1.91 Å with an interplane angle of 66° can be indexed to the (110) and (018) planes of rhombohedral calcite. Likewise, the d-spacings marked in (f) measuring A: 5.77 Å and B: 2.41 Å with an interplane angle of 88° could be indexed to the (001) and (200) planes of orthorhombic aragonite, respectively.

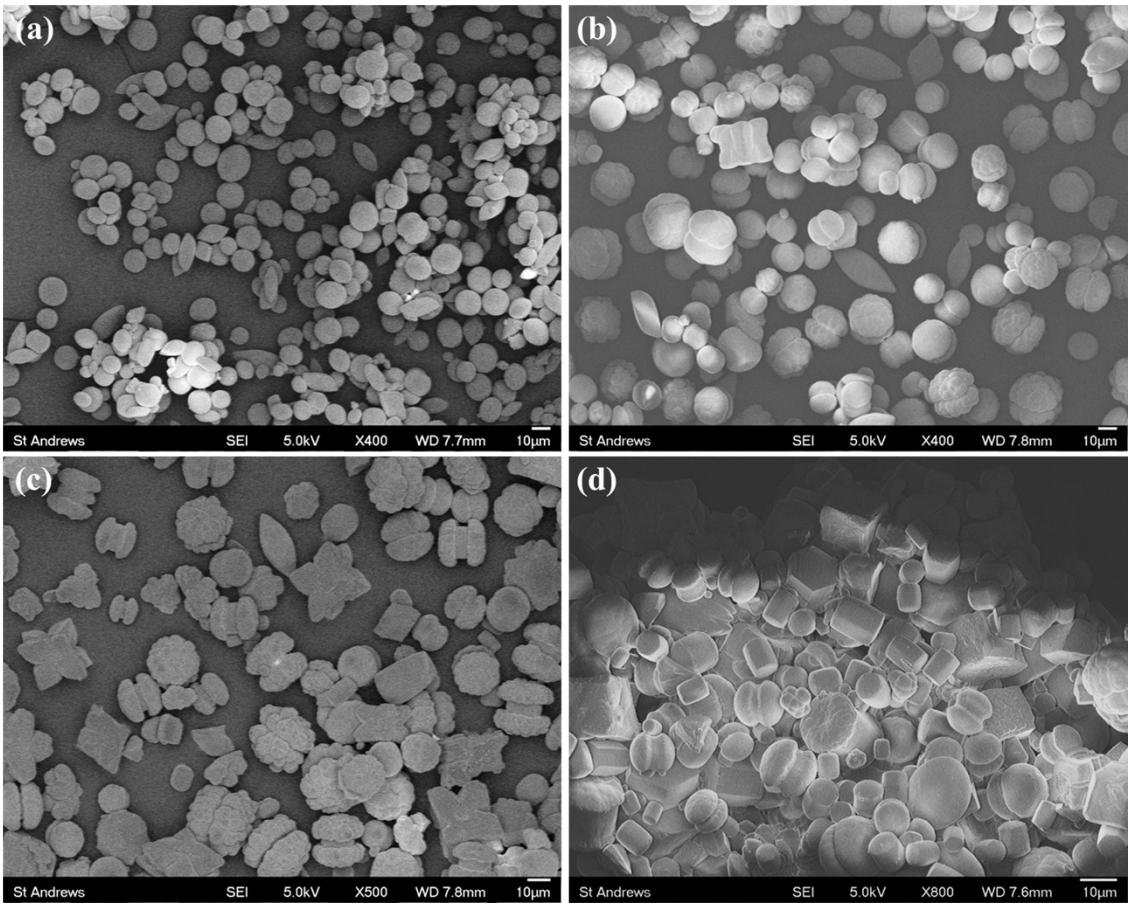

Fig. S2 Low magnification SEM image of (a) 3 h, (b) 6 h, (c) 23 h and (d) 96 h specimens prepared using 5.71 M urea and 28 g/L of gelatin.

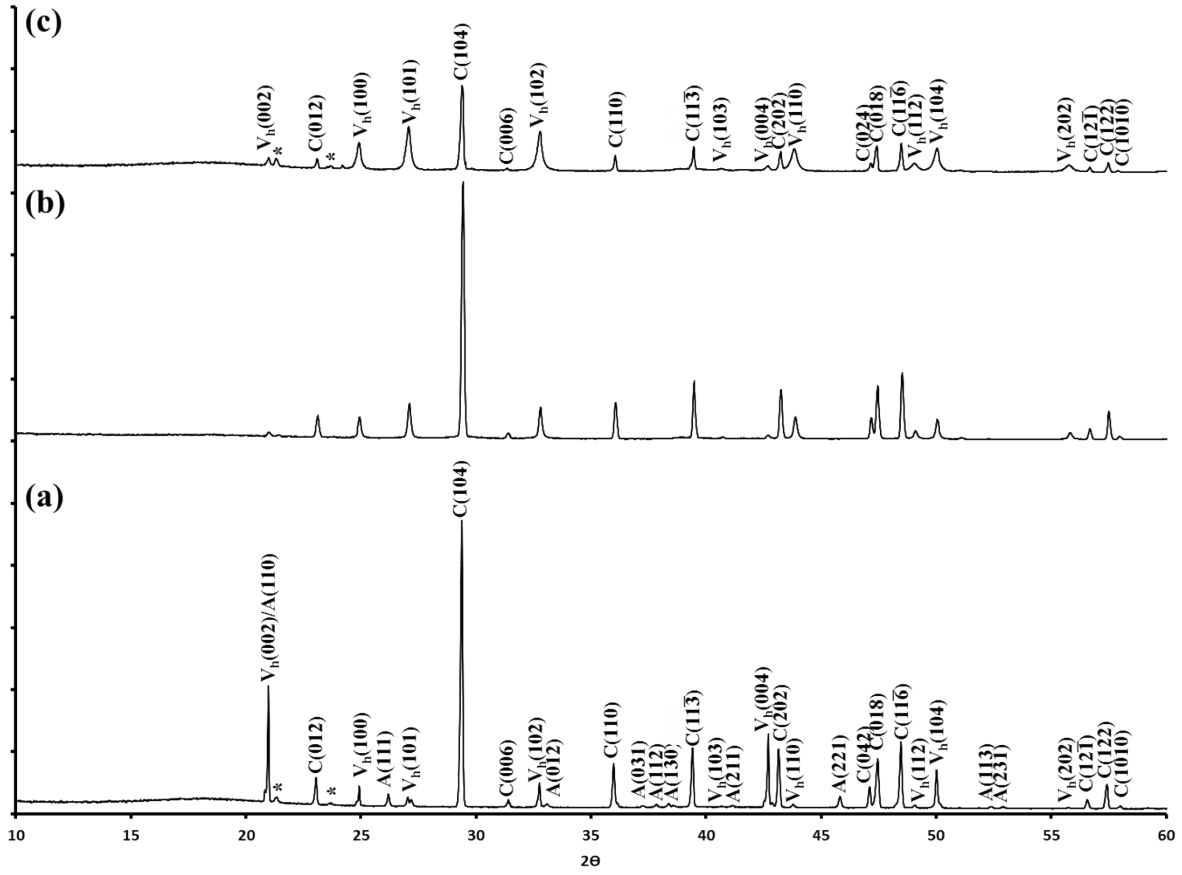

Fig. S3 PXRD patterns of 23 h specimens prepared using 5.71 M urea and varying gelatin concentrations of (a) 0 g/L, (b) 7 g/L, and (c) 28 g/L. PXRD patterns (a) and (c) are indexed to the hexagonal vaterite phase, rhombohedral calcite phase and orthorhombic aragonite (denoted V_h, C and A) crystal structures, respectively. The peaks marked by * in (a) and (c) correspond to columnar peaks from the diffractometer.

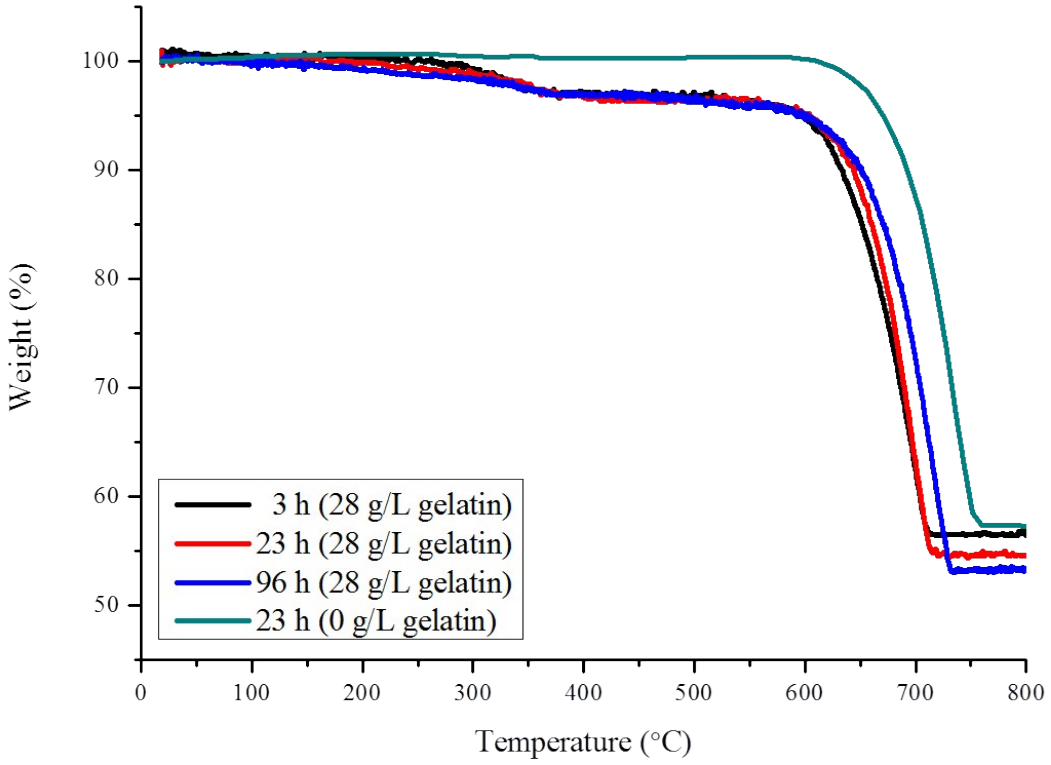

Fig. S4 TGA results of 3 h, 23 h and 96 h specimens prepared using 5.71 M urea and a gelatin concentration of either 0 or 28 g/L. All specimens had a mass loss of ~40 wt% observed between 560 and 750°C corresponding to the decomposition of vaterite into CaO and CO_2. PXRD patterns (not shown) of specimens after heating to 750°C under N_2 confirmed all $CaCO_3$ polymorphs decomposed into a pure CaO phase with a cubic unit cell, (JCPDS 82−1691) a = 4.796 Å, space group $Fm\bar{3}m$. Specimens containing gelatin had an initial mass loss of approximately 2.75 wt% between 250 and 360°C caused by the elimination of organic groups (usually proline) in gelatin whilst the second mass loss of 37 wt% observed between 600 and 705°C in the 3 h specimen and 41 wt% weight loss between 600 and 730°C in the 96 h specimen occurred from the decomposition of the $CaCO_3$ polymorphs. The end wt% point of the gelatin containing specimens have terminal weights varying by <2 wt% between each specimen due to the thermal decomposition of the amino acid glycine in gelatin. Literature suggests this occurs between 540 and 600°C.[1] From these terminal weights it can be assumed that the 96 h specimen contains 1.7 wt% more gelatin than the 23 h specimen which in turn contains 1.8 wt% more gelatin than the 3 h specimen. The wt% embedded gelatin within the $CaCO_3$ particles in the 3 h, 23 h and 96 h specimen was calculated as 6.1 wt%, 7.8 wt% and 9.5 wt%, respectively. The higher temperature required to complete the decomposition of the 96 h specimen into CaO and CO_2 compared to the 3 h and 23 h specimens can be explained from the later samples containing much more densely packed structures which makes decomposition increasingly difficult.

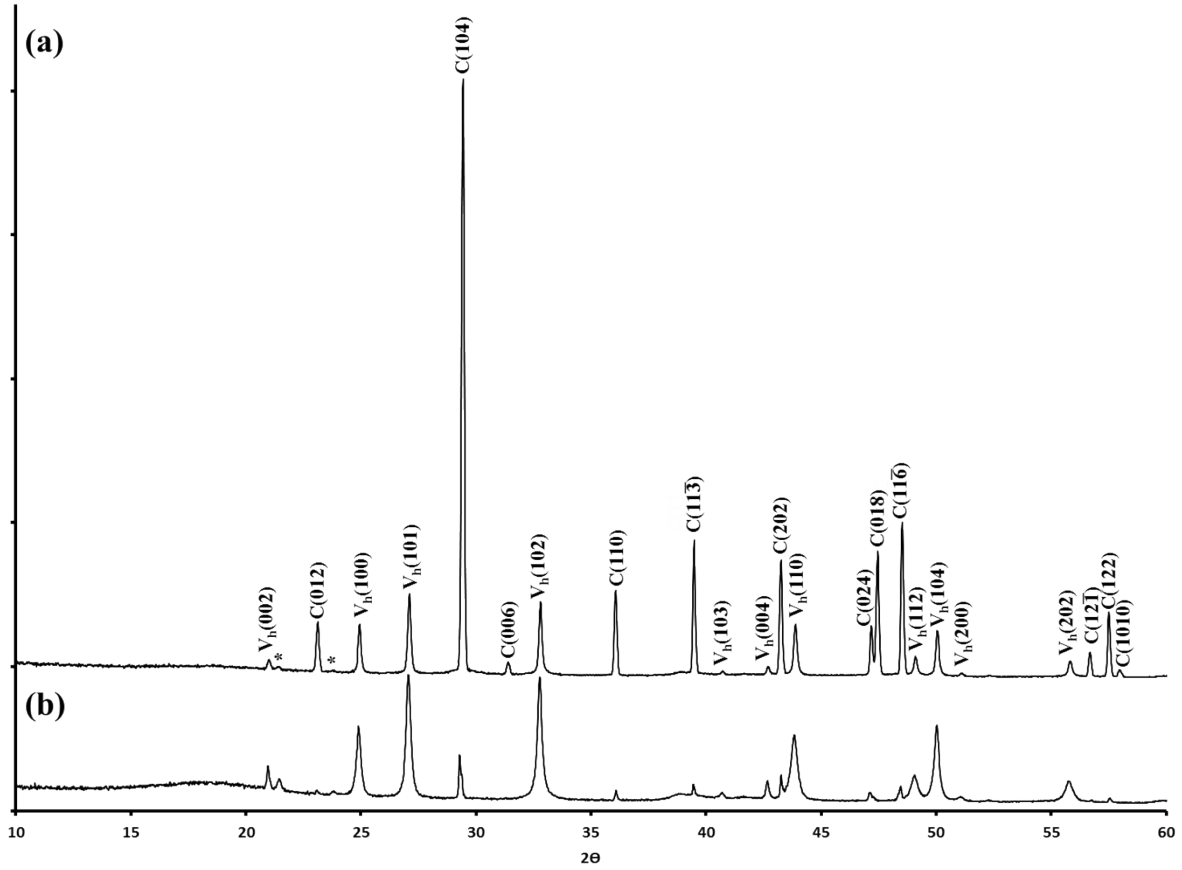

Fig. S5 PXRD patterns of 6 h specimens prepared using 28 g/L gelatin and urea concentrations of, (a) 2.86 M, and (b) 5.71 M. PXRD pattern (a) is indexed to the hexagonal vaterite phase (V_h) and rhombohedral calcite (C) crystal structures, respectively. The peaks marked by * in (a) correspond to columnar peaks from the diffractometer.

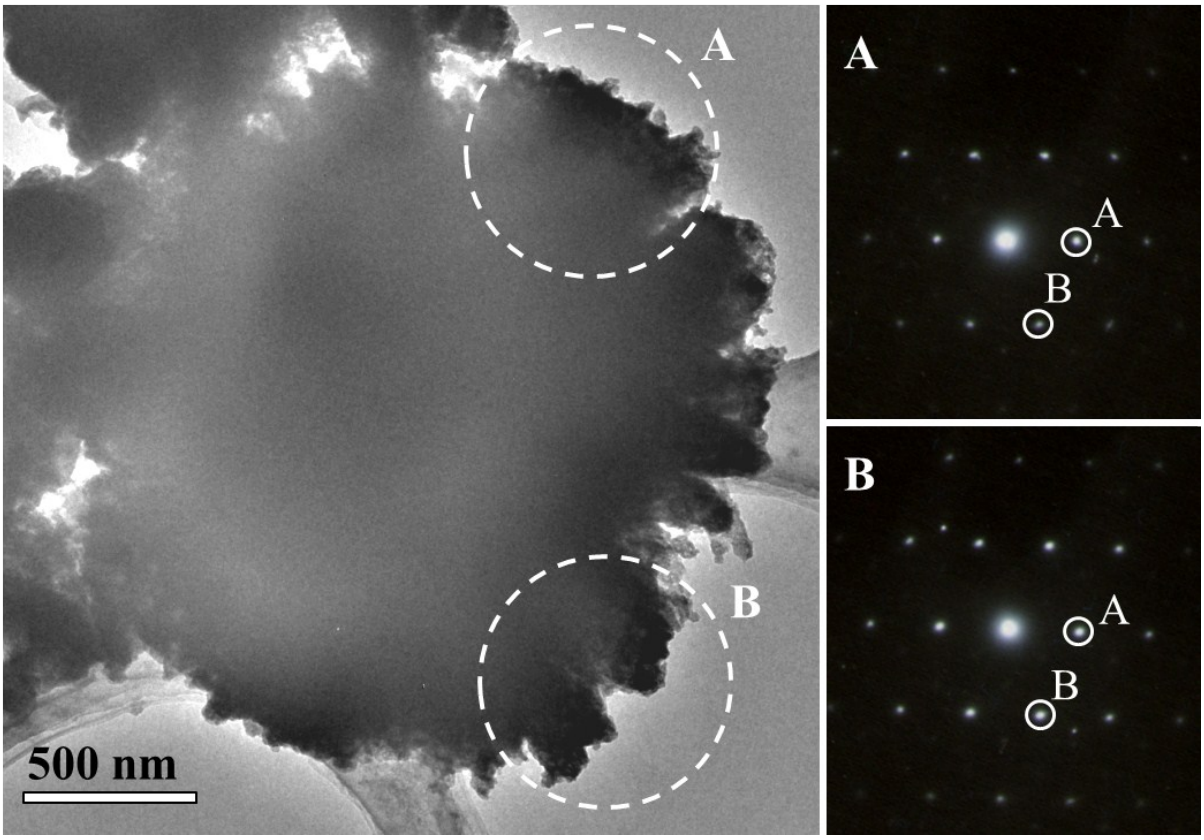

Fig. S6 TEM image of a spherulite particle found in the 6 h specimen (28 g/L gelatin, 2.86 M urea). Single crystalline-like SAED patterns recorded from the areas marked A and B, respectively. Both SAED patterns are identical confirming all nanocrystallites within a spherulite type crystal have exactly the same orientation. D-spacings measured from the spots marked A and B were 3.54 Å and 2.72 Å with an interplane angle of 67°. These could be indexed to the (100) and (012) planes of hexagonal vaterite.

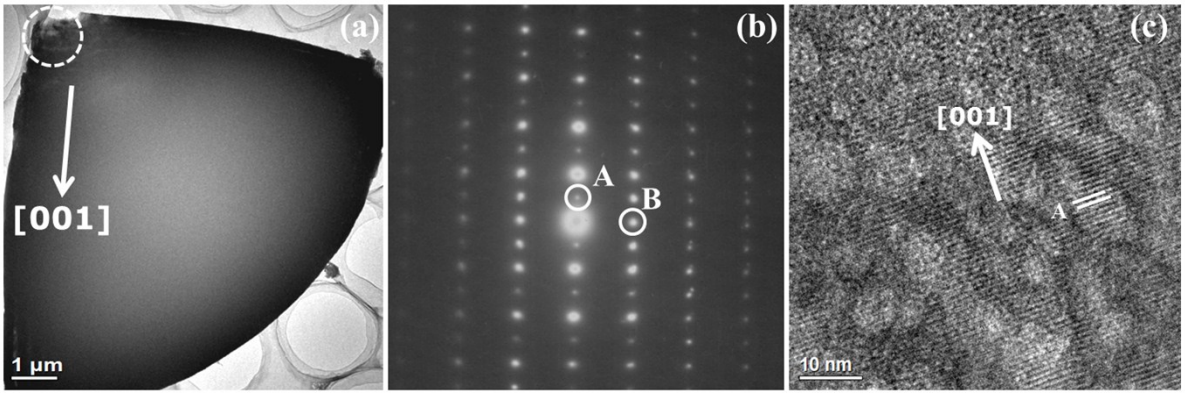

Fig. S7 (a) TEM image of a broken ellipsoid particle. (b,c) SAED pattern and HRTEM image recorded from the region located within the circle in (a). D-spacings measured from the marked diffraction spots in (b) are A: 7.99 Å and B: 3.34 Å which can be indexed to the (001) and (100) crystal planes of hexagonal vaterite. The lattice fringes in (c) measuring A: 8.54 Å can also be indexed to the (001) planes of vaterite. The indexing in (b,c) confirmed the longest dimension of the ellipsoid particle is parallel to the [001] zone axes as demonstrated by the arrow in (a).

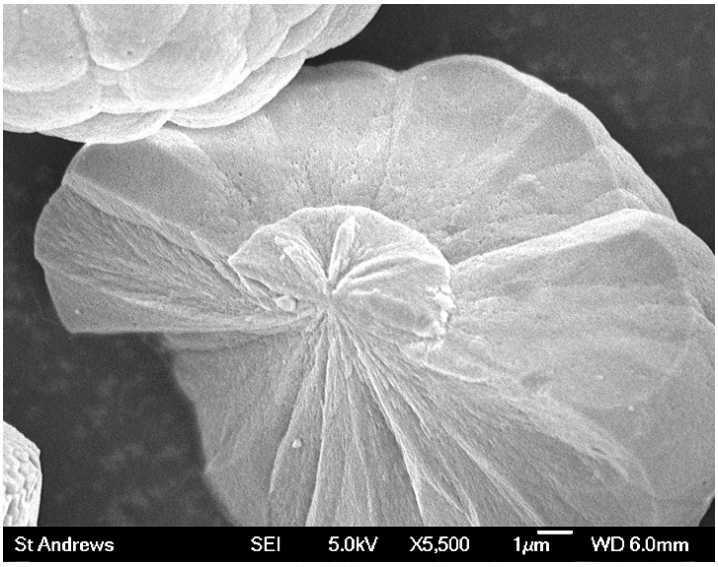

Fig. S8 SEM image of a broken twin cauliflower-like particle revealing a small disc in the core.

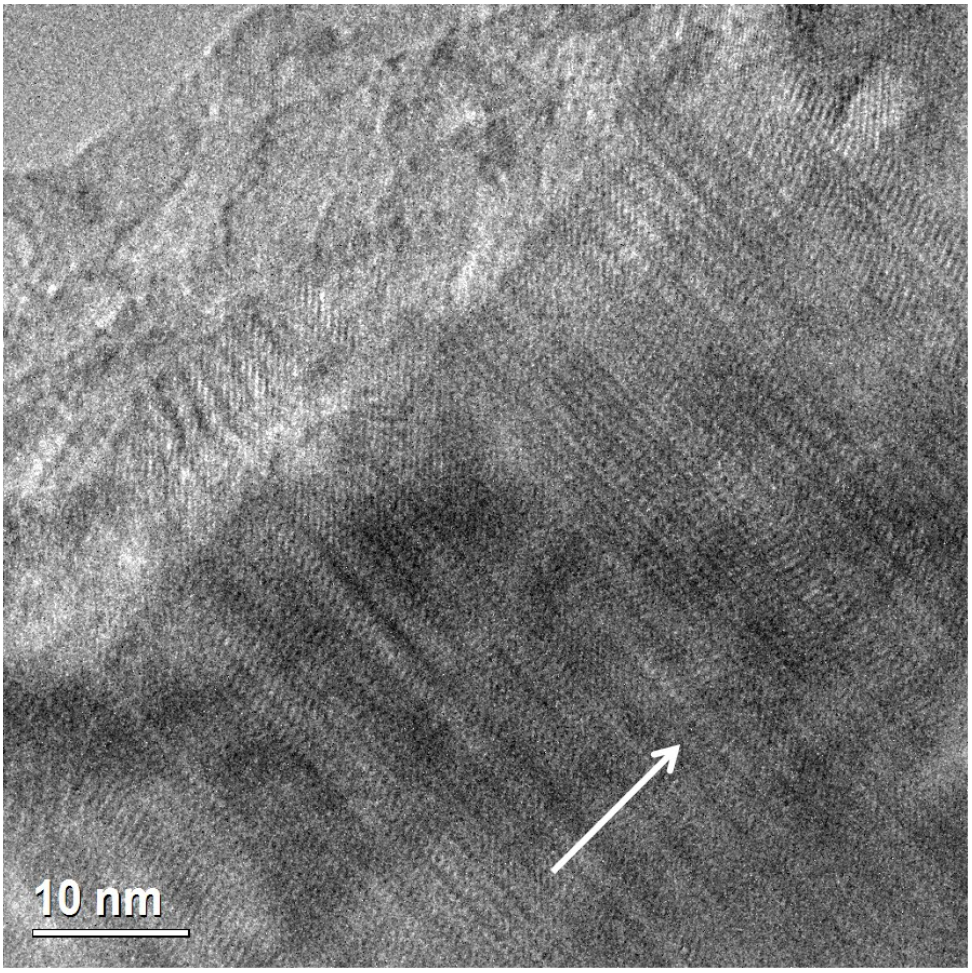

Fig. S9 HRTEM image of the hexagonal prism particle shown in **Fig. 6f**, showing defects and an incommensurate superstructure. The arrow indicates the [001] direction.

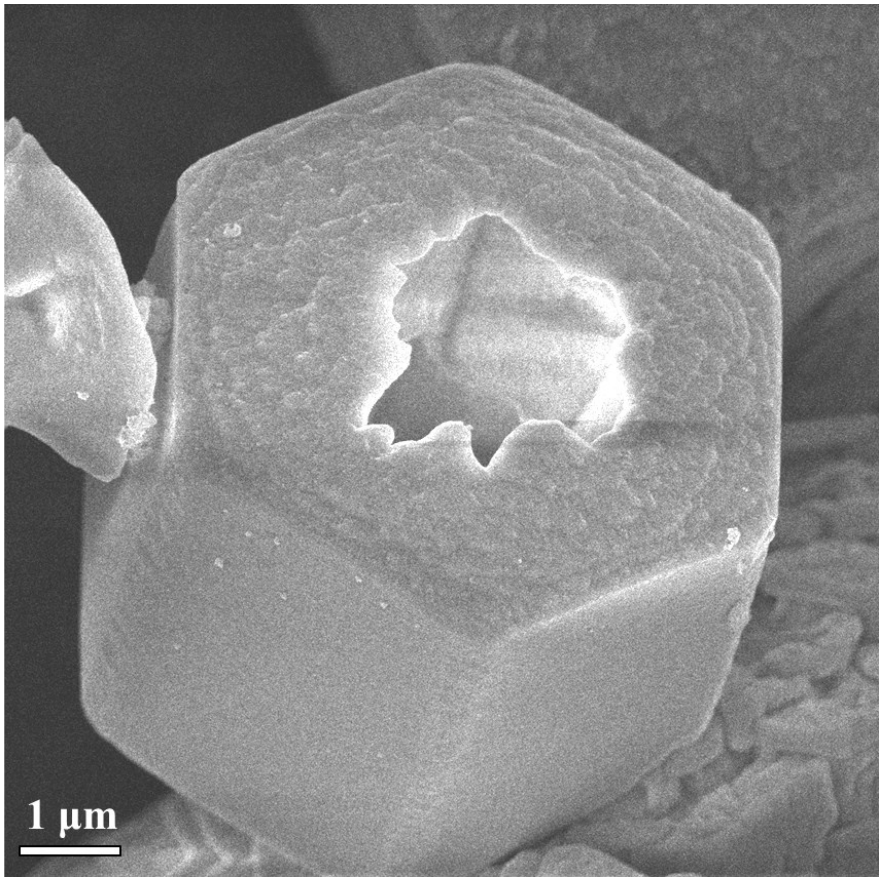

Fig. S10 SEM image of a hollow hexagonal prism vaterite particle prepared when the 96 h specimen was treated in acidic conditions (pH 3) under hydrothermal conditions for 3 h.

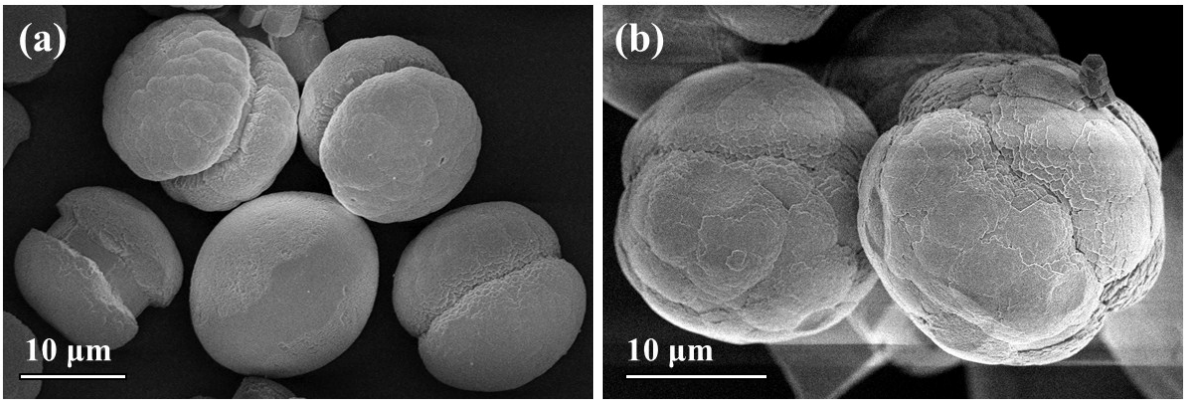

Fig. S11 SEM images of vaterite particles prepared in gelatin solution (28 g/L) with the addition of KCl at concentrations of (a) 0.14 M and (b) 0.57 M, respectively. Both specimens were collected after a hydrothermal treatment time of 96 h.

REFERENCE

(1) A. S. De Menezes, C. M. R. Remédios, J. M. Sasaki, L. R. D. da Silva, J. C. Góes, P. M. Jardim and M. A. R. Miranda, *J. Non-Cryst. Solids*, 2007, **353**, 1091.